The use of automatic scale selection to improve the spatial and spectral resolution of a scintillator-coupled EMCCD

Journal Item

The use of automatic scale selection to improve the spatial and spectral resolution of a scintillator-coupled EMCCD

David J. Hall [a,*] Andrew Holland [a] David R. Smith [b]

[a] *Planetary and Space Sciences Research Institute, Open University, Walton Hall, Milton Keynes MK7 6AA, UK*
[b] *Imaging for Space and Terrestrial Applications, School of Engineering and Design, Brunel University, Uxbridge, UB8 3PH, UK*

Abstract

The technology behind the Electron-Multiplying Charge Coupled Device (EMCCD) was successfully exploited by e2v technologies in the late 1990s. Since then, many uses have been found for these low light level (L3) devices including surveillance and many scientific applications. The EMCCD increases or 'multiplies' the charge signal by the phenomenon of impact ionisation (or avalanche multiplication) allowing the detection of low signal events of only a few photons. When coupled with a scintillator, this low light capability can be used to image photon flashes from individual X-ray interaction events. The combination of depth of interaction effects in the scintillator, shot noise on the signal and the multiplication noise factor lead to large variations in the profile of the detected signal from a constant energy X-ray source. This variation leads to reduced spectral performance and can have adverse effects on the centering techniques used in photon-counting imagers. The concept of scale-space is similar in many ways to the Fourier or Wavelet Transforms. Automatic scale selection can be implemented through the scale-space transform as a method of fitting a known profile to the observed photon flash. The process is examined here in the context of the photon-counting EMCCD detector and the results obtained in both simulated and experimental data compared. Through the analysis of the fitting process and the results achieved, the implications on imaging performance and spectral resolution are discussed.

Key words: Photon counting, scintillator, EMCCD, Geant4, scale-space, automatic scale selection

1. Introduction

The X-ray/gamma camera has many uses in medical physics, namely in Single Photon Emission Computed Tomography (SPECT). Improvements in spatial resolution can lead to great advancements in the merit of SPECT imaging systems. The ability to discriminate between X-rays of different energies has not been possible with basic analysis techniques due to the complicating factors in depth of interaction effects and the various noise factors on the imaging system. Here, an alternative analysis process is described with the aim of not only allowing removal of all non-X-ray-like events but to also develop a multi-label imaging system with the use of several radioisotopes.

2. The photon counting gamma camera

Until recently, the standard gamma camera consisted of an array of photo-multiplying tubes, coupled to a scintillation layer. The spatial resolution of such a camera is limited by the geometry of the photo-multiplier tubes used. Developments in EMCCDs have enabled the birth of a new breed of gamma cameras, using scintillators coupled to EMCCDs. The limits on the spatial resolution are now dominated by the spread of light in the scintillator. The scintillator, CsI(Tl), can be grown to give a collimated structure with columns of a few micrometers in diameter. The columns, although not perfect, act to channel to the light by total internal reflection, reducing the spread of light in the scintillator.

The photon-counting gamma camera is designed to resolve individual X-ray interactions in the scintillator. Many frames are taken in which only tens of events occur. An event is defined here as the Gaussian-like signal seen over several pixels relating to the visible photons produced in an X-ray interaction in the scintillator. The EMCCD allows these small signals to be multiplied before output, increasing the signal to noise ratio and allowing the individual events to be resolved above the background.

Centering techniques can be used on the individual events to more precisely locate the X-ray interaction,

* Corresponding author.
Email address: d.j.hall@open.ac.uk (David J. Hall).

leading to improved intrinsic spatial resolutions of below 50 µm [1].

The photon output from CsI(Tl) is approximately 52 photons (∼550 nm) per keV. As the photon output scales with the energy of the incident X-ray, attempts have been made to use energy discrimination [2].

2.1. *Limits on resolution*

Spatial resolution can be deteriorated by the inclusion in the image of scattered X-rays and the K X-rays from the Cesium and Iodine [3]. Regions of random bright pixels can also degrade the spatial resolution achieved. The spectral resolution of the photon-counting camera has been severely limited in previous studies by depth of interaction (DOI) effects. The depth of the X-ray interaction in the scintillator layer determines the event profile recorded by the EMCCD. X-rays interacting far from the EMCCD are subject to greater spread and hence a lower peak intensity. Ignoring these DOI effects leads to severely limited energy resolutions of the order of the energy of the interacting X-ray [3] and attempts to sum the signal over several pixels appear to give little improvement [4].

The shot noise on the low signal events can also act to deteriorate both the spatial and spectral resolution. The brightest pixel in an event is no longer necessarily the central pixel. The variation in signal level for events of the same DOI due to the shot noise leads to the spreading of the spectral peak. Furthermore, the multiplication of signal in an EMCCD is not an exact process. The gain achieved is an average value per pixel and the actual gain may be described by the Poisson distribution, leading to an additional multiplication noise factor of 2 at high gain [5].

2.2. *Spectral and spatial resolution*

The methods described in this paper aim to reduce the impact of the limiting factors described above. By fitting a profile to each event, shot noise on the signal and the multiplication gain can be averaged out. The event profile can then be used to determine not only the spatial position of the event, but also the energy of the event. The DOI effects can be accounted for through the use of both the intensity and spread of each event.

At the low signal levels required in these measurements (a few photons), fitting a Gaussian-like profile through standard fitting procedures is inefficient due to the noise on the signal.

3. Scale-space

Just as the Fourier transform or wavelet transform allow analysis of one-dimensional waveforms, scale-space theory can be used to analyse a two-dimensional image.

For a given grayscale image, $I(x, y)$, a scale-space representation can be produced, $L(x, y; \sigma_k^2)$, through the convolution of the image I with progressive Gaussian kernels of scale σ_k^2, where σ_k is the standard deviation of the Gaussian kernel [6]:

$$L(x, y; \sigma_k^2) = \frac{1}{2\pi\sigma_k^2} \exp\left(-\frac{x^2 + y^2}{2\sigma_k^2}\right) * I(x, y) \tag{1}$$

The response of an artifact in the image is dependent upon the scale of the artifact. For a Gaussian-like artifact in the image I, the response in scale-space is given below, where σ_k^2 is the variance of the kernel and σ_i^2 is the variance of the image artifact.

$$L(x, y; \sigma_k^2) = \frac{A\sigma_i^2}{\sigma_i^2 + \sigma_k^2} \exp\left(-\frac{x^2 + y^2}{2(\sigma_i^2 + \sigma_k^2)}\right) \tag{2}$$

3.1. *Automatic scale selection*

When a Gaussian-like artifact is traced through scales in L, the scale of the artifact itself can be calculated. The trace of the normalised Hessian matrix, H_{norm}, can be applied to L through all scales to give J [6]:

$$J(x, y; \sigma_k^2) = \mathrm{tr}(H_{norm})L = \sigma_k^2 \left(\frac{\partial^2}{\partial x^2} + \frac{\partial^2}{\partial y^2}\right) L \tag{3}$$

The function $J(\sigma_k^2)$ has a turning point, occurring where the derivative of J with respective σ_k^2 is equal to zero. The turning point occurs when the scale of the image artifact matches the scale of the Gaussian kernel, when σ_k is equal to σ_i.

Once the coordinates of a point of interest, (p, q), have been specified, the scale of the image artifact can be determined through the calculation of $J(p, q)$ and the fitting of the parameters A, the peak intensity, and σ_i^2, the scale of the image artifact:

$$J(p, q) = -2A\frac{\sigma_i^2\sigma_k^2}{\sigma_i^2 + \sigma_k^2} \tag{4}$$

This method of event profile fitting allows noisy data to be analysed to signal to noise levels orders of magnitude lower than can be achieved with standard fitting procedures.

4. Simulated results

A simulation was designed to give the signal photons expected to arrive at the detector surface in a perfect environment. Through the study of the noise-free scenario, the basic design of the system and the method of analysis can be developed.

The simulation geometry consists of a collimated Cesium Iodide scintillation layer, with scintillation columns of width 6 µm and separation 1 µm. The properties of the layer were defined to match those expected for the real scintillation layer.

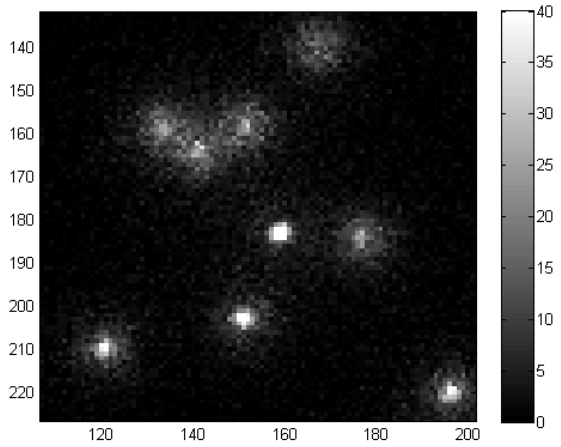

Fig. 1. A section of a simulated image for 60 keV incident X-rays. The intensity scale gives the number of photons detected per pixel. Clear differences can be seen in the spread and brightness of each event. Interactions furthest from the detector surface have the larger spread and lower central brightness.

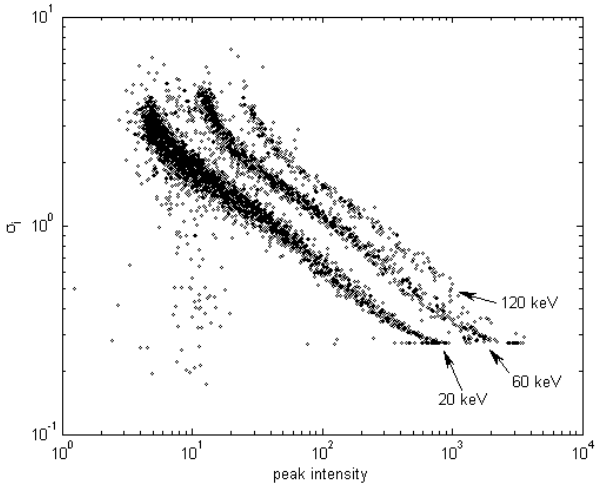

Fig. 2. A peak versus spread map of simulated events produced by X-ray interactions in the scintillator of energy 20 keV, 60 keV and 120 keV.

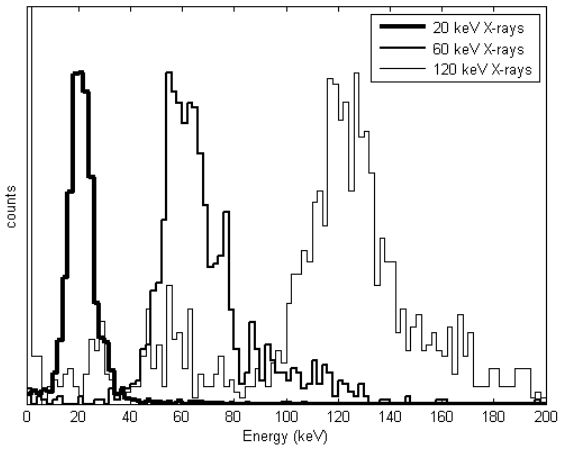

Fig. 3. A histogram of the 'energy' of events, produced using the peak intensity multiplied by σ_i^2. This analysis assumes a Gaussian-like profile, fitting the simulated data.

4.1. *X-ray interaction events*

The simulation results show clearly the differing image profiles that occur with different X-ray interaction depths in the scintillator, Figure 1. The differing profiles, all for the same energy of incident X-ray, show how the energy of the interacting X-ray cannot be assumed purely from the measured peak intensity.

4.2. *Spectroscopic measurements*

Applying the automatic scale selection method described in Section 3 allows generation of a 'peak versus spread' map of the X-ray interaction events. Typical energies of 20 keV, 60 keV and 120 keV were simulated, approximately representing ^{125}I, ^{241}Am and ^{57}Co respectively, Figure 2 and Figure 3.

Although it is not expected that the low-signal tails of an event may be accurately measured from the background or shot noise, the peak and spread of the event profiles can be used to create a histogram of the 'energy' of the interacting X-ray.

5. Experimental device

The experimental arrangement consists of a CCD97 L3 EMCCD from e2v technologies coupled directly to a fibre-optic plate. A secondary fibre-optic plate is coupled directly to a layer of CsI(Tl) which has been grown with a collimated structure. The secondary fibre-optic plate is clamped against the fibre-optic plate of the CCD97 while measurements are taken. This arrangement allows for the testing of different scintillator types and structures in future measurements.

6. Initial results

The device described in Section 5 has been used to acquire preliminary images of events relating to a 60 keV ^{241}Am X-ray source. The initial analysis of the acquired images is detailed here.

6.1. *Form of photon interaction*

The 'peak versus spread' map of the experimental data shows a grouping similar to that predicted by the simulation, Figure 4. The corresponding 'energy' spectrum is shown in Figure 5. The high energy tail to the energy spectrum is currently being investigated and can be seen to the upper right of the main grouping in Figure 4.

The lower region of the map in Figure 4, labeled 'bright pixels', can easily be distinguished from the main event

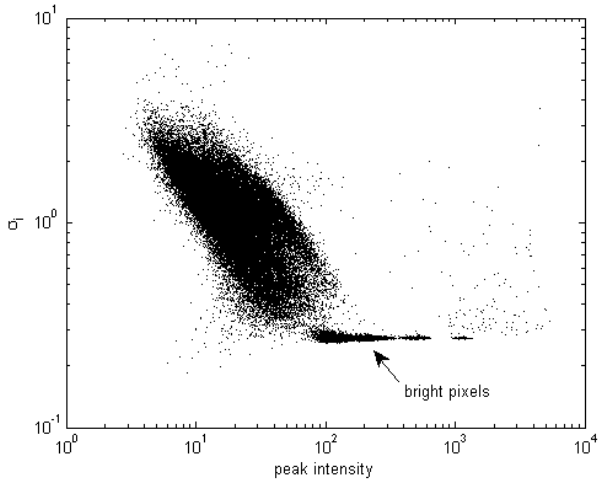

Fig. 4. A 'peak versus spread' map of real events produced by X-ray interactions in the scintillator of energy 60 keV. Bright pixels can be clearly isolated from the event data.

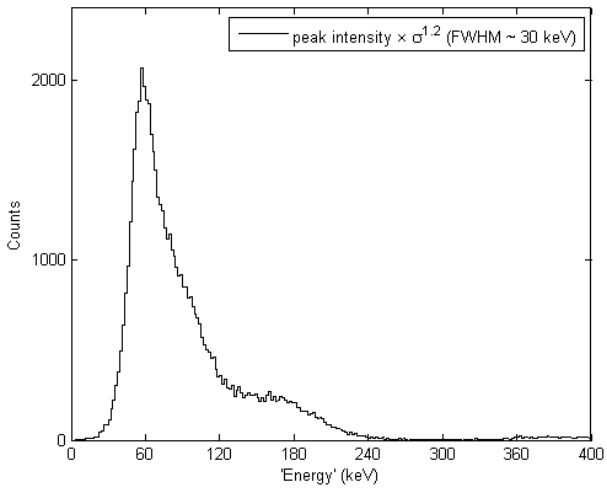

Fig. 5. The 'energy' spectrum taken from the initial experimental data.

data. This allows false events due to bright pixels and regions of higher noise to be excluded from the data. A point of interest arises in the difference between the simulated and real data. The map for the real data shows a different gradient to the simulated results. This could be explained by several theories. The imperfect collimation in the real CsI(Tl) could lead to a non-Gaussian profile of the form:

$$f(x) \sim \exp\left(-\frac{x^2+y^2}{2\sigma^p}\right) \quad (5)$$

where p is approximately 1.2 from current data. Alternatively, a doping gradient in the CsI(Tl) could cause a shift in the number of photons produced depending on the depth in the scintillator. As the spread of the event is a measure of the depth of interaction, this could act to 'tilt' the profile.

The possible causes for these discrepancies are being investigated along with work to improve the grouping of the events, as this directly relates to the spectral resolution.

6.2. *Improvements on spatial and spectral resolution*

The energy spectrum shown in Figure 5 shows a histogram for the new scale-space energy determination method. The FWHM is currently approximately 30 keV, although this data was produced without optimisation of the image system or analysis method. Figure 4 shows how bright pixels and non-X-ray-like events can be removed instantly from their position in the 'peak vs spread' map. This simple discrimination improves the image spatial resolution by removing non-events and removes the same non-events from the energy spectrum.

With further improvements to the image acquisition and data analysis it is hoped that it will be possible to discriminate between events of differing energies and hence remove events due to scattered X-rays and K X-rays. Energy discrimination should enable the use of multi-label imaging systems where events arising from different X-ray sources may be distinguishable.

7. Conclusions

The automatic scale selection process allows individual X-ray detection events to be classified by the peak intensity and spread of the signal. This allows event discrimination to be implemented to remove bright pixels and other such non-X-ray-like events to improve spatial resolution. The implications from the simulated and early experimental data lead to the possibility of a multi-label imaging system, further advancing the use of the scintillator-coupled EMCCD system in medical imaging.

Acknowledgements

With thanks to Bill Bruns, Peter Pool and Mark Robbins of e2v technologies ltd for their help and advice on the EMCCD and scintillator and for providing the CCD97 and CsI(Tl) used in the experimental work, and with thanks to David Burt of e2v technologies ltd for general discussion.

References

[1] J.W.T. Heemskerk, A.H. Westra, P.M. Linotte, K.M. Ligtvoet, W. Zbijewski, F.J. Beekman, IOP Physics in Medicine and Biology 50 no. 8 (2007) N149.
[2] B.K. Teo, I. Shestakova, M. Sun, W.C. Barber, B.H. Hasegawa, V.V. Nagarkar, IEEE Transactions on Nuclear Science 53 no. 5 (2006) 2495
[3] B.W. Miller, H.B. Barber, H.H. Barret, I. Shestakova, B. Singh, V.V. Nagarkar, Proceedings of the SPIE 6142 (2006) 642.
[4] I. Shestakova, V.V. Nagarkar, V. Gaysinskiy, G. Entine, B.C. Stack, B. Miller, Proceedings of SPIE 6319 (2006) 63191E.1.
[5] M.S. Robbins, B.J. Hadwen, IEEE Transactions on Electron Devices 50 (2003) 1227
[6] T. Lindeberg, Int. J. of Computer Vision 30 no. 2 (1998) 117